Received: 12 June 2019 | Revised: 13 August 2019 | Accepted: 13 September 2019
DOI: 10.1002/mmce.21993

RESEARCH ARTICLE

INTERNATIONAL JOURNAL OF RF AND MICROWAVE COMPUTER-AIDED ENGINEERING WILEY

Long read range and flexible UHF RFID tag antenna made of high conductivity graphene-based film

Bohan Zhang[1,2] | Xuyang Tang[2] | Jingwei Zhang[2] | Chengguo Liu[2] | Daping He[2] | Zhi P. Wu[1,2]

[1]School of Information Engineering, Wuhan University of Technology, Wuhan, China
[2]Hubei Engineering Research Center of RF-Microwave Technology and Application, Wuhan University of Technology, Wuhan, China

Correspondence
Bohan Zhang, School of Information Engineering, Hubei Engineering Research Center of RF-Microwave Technology and Application, Wuhan University of Technology, Wuhan 430070, China.
Email: zhangbohan@whut.edu.cn

Abstract
An antenna made of a graphene-based film with organic polyimide precursor of high conductivity 1.1×10^6 S m^{-1} and thickness 30 μm, operating in the ultrahigh frequency (UHF) band for radio frequency identification applications is presented in this article. The antenna is optimized to have a conjugate match to the impedance of the chip by tuning the design parameters. Tags are fabricated and tested using the designed antenna, which are shown to have realized gain above −1.5 dBi and radiation efficiency beyond 90% in the whole UHF band from 860 to 960 MHz. The read range of proposed tag is greater than 12.3 m over the entire UHF band with a maximum value of 14 m at 920 MHz. In addition, the flexibility of the tags is demonstrated. After 2000 cycles of bending and stretching, the read range only decreases by 4.5 m comparing to the initial state at 915 MHz.

KEYWORDS
flexible, graphene-based film, high conductivity, long read range, UHF RFID

1 | INTRODUCTION

In recent few years, radio frequency identification (RFID) technology has attracted tremendous attention due to the rapid development of Internet of Things (IoT) applications in the 5G communication era.[1,2] The RFID technology at the most front end of information collection plays a fundamental role in the IoT. RFID tags in the ultrahigh frequency (UHF) band have passive, wireless, medium read range, unique identification properties, and low-cost feature. Antenna is a key component of an RFID tag.[3,4] Current antenna fabrication mainly uses a metallic material as the conductive element, but this process is complicated and expensive. Moreover, the metallic antennas are prone to oxidation, corrosion, and poor flexibility. As a result, many different types of novel materials are emerging for antenna technology.

Among these materials, conductive polymers,[5,6] carbon nanotubes,[7,8] graphene,[9,10] and graphene-based composites[11-16] are very promising due to their special physical and excellent electrical properties. However, there are many challenges of using these materials for antenna design and fabrication. Compared with metals, the conductivities of these materials are relatively low, resulting in poor radiation efficiency. Even with the highest conductivity (~10^8 S m^{-1}), graphene is not a good candidate as a conductor material for antenna design in the microwave range, because of the very high sheet resistance (~30 Ω) and high ohmic loss caused by the extremely thin 2D atomic structure (0.34 nm). Graphene discovered by Geim and Novoselov in 2004 can be applied for a variety of advanced applications, including EMI shielding and antenna design.[9] The monolayer and few layer graphene appears more appropriate in terahertz (THz) range than microwaves.[10] In contrast to monolayer and few layer concepts, graphene-based composites materials made of graphene-related materials have been realized and produced in large scale. Graphene inks as graphene-based composites have also been proven in numerous studies for RFID applications.[11] However, graphene inks generally contain at least one kind of binder and dispersant to form a continuous film, these will reduce the ink conductivity.[12] The use of RFID antennas made of low conductivity materials leads to a short read range of 4 to 5 m and low radiation efficiency of 40% to 50%.[14,15]

In this article, we proposed a long read range and flexible UHF RFID tag antenna made of a graphene-based film with organic polyimide precursor. The conductivity of graphene-based film is 1.1×10^6 S m^{-1}, which is comparable to the metal and nearly two orders of magnitude higher than previously reported graphene-based composites (The corresponding sheet resistance is 0.03 Ω sq^{-1}, which is two orders of magnitude lower.).[13-16] The RFID antenna is designed and optimized by tuning the parameters through simulation software and conjugate matching to the impedance of the chip. The tags with optimized antenna parameters and those with unoptimized antenna parameters are fabricated, and the simulated and measured properties of tags are presented, including the realized gain, radiation efficiency, and read range. Further details are given below.

2 | TAG FABRICATION

As a new material for RFID application, the formation of the conductive graphene-based film in this article is made through the thermal treatment of organic polyimide precursor.[17,18] The polyimide precursor is slowly heated to 1200°C to 1400°C in vacuumed electric furnace for 5 to 8 hours, in order to decompose noncarbon atoms and form the carbonized structure. The carbonized structure is fired at an ultrahigh temperature of 2800°C to 3000°C under Ar gas flow to form the graphitized structure with complete c—c sp2 hybridization. The graphitized structure is then passing through rolling process to get high oriented and densely packed structure graphene-based film. The cost of graphene material is generally lower than metal. The use of polyimide precursor-based process, not only reduces the fabrication cost, but also makes films with large areas possible. The conductivity (σ) and sheet resistance (R_s) of the graphene-based film are measured by using a four-point probe resistance measurement system. The graphene-based film on the polyethylene terephthalate (PET) substrate is shown to be flexible in Figure 1A. The antenna made of graphene-based film is patterned accurately using an LPKF laser machine rather than traditional metal etching, which is simple and environmentally friendly. The adhesive dispending and flip chip bonding is done by semiautomatic packaging machine. Finally, the tag can be placed on different substrates including PET, textile, plastic, cardboard, and glass for various application scenarios. The following read range tests, unless otherwise specified, are all theoretical read range measurements of the tags on PET substrate. The tag measurements are conducted by using *Voyantic Tagformance Pro RFID measurement system* in anechoic chamber, as shown in Figure 1B.

3 | ANTENNA DESIGN AND OPTIMAZATION

In the design of tag antennas, the power transfer efficiency τ representing the fraction of power transfer from antenna to chip is a crucial parameter, which is calculated by:

$$\tau = |s|^2 = \left|\frac{Z_c - Z_a^*}{Z_a + Z_c}\right|^2 = \frac{4R_aR_c}{|Z_a + Z_c|^2} \quad 0 \le \tau \le 1 \qquad (1)$$

The reflection coefficient s describes the mismatch between the antenna impedance ($Z_a = R_a + jX_a$) and the chip impedance ($Z_c = R_c + jX_c$). According to the conjugate matching principle, the power delivered to the chip is maximized with $Z_a = Z_c$*. For the chips of Impinj Monza R6

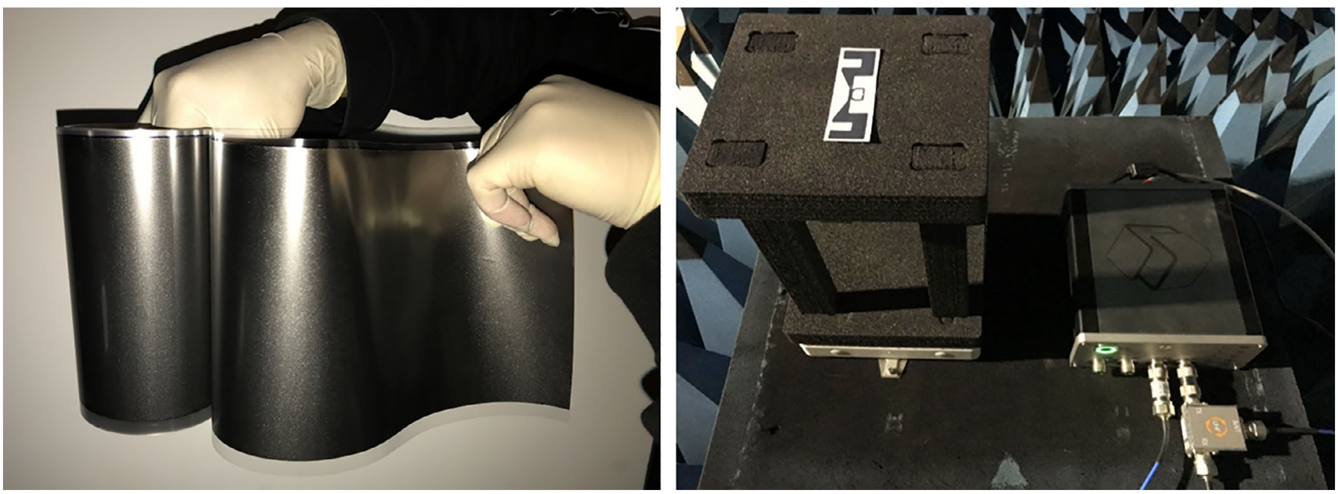

FIGURE 1 A, The flexible graphene-based film on PET substrate. B, The system for the measurement of tag in anechoic chamber

series used, the chip impedance is 12-j 119.6 Ω at the operating central frequency 915 MHz.

The geometry of the proposed tag antenna made of graphene-based film is shown in Figure 2. The tag represents one of the design types in the dogbone family.[19] The modeling of the antenna is made through a piece of full wave simulation software. The PET substrate used to support the antenna has thickness of 0.05 mm, dielectric constant of 3.9, and tangent loss of 0.003.

In order to investigate the effects of different loop length (l_1) on the antenna impedance, l_1 is increased from 3.5 to 4.5 mm in a step of 0.5 mm while other parameters are kept constant. The calculated conjugate impedance of R6 chip and the simulated impedances of antenna for different l_1 vs frequency are shown in Figure 3A. With l_1 increasing, it can be observed that the antenna resistance increases from 9.9 to 14.5 Ω and the antenna reactance increases from 109.5 to 130.3 Ω at the resonant frequency of 915 MHz, respectively. Since l_1 controls loop size as well as coupling area, l_1 affects both the real and imaginary parts of the impedance. It is evident from the curves that the red one has intersections with the chip conjugate impedance at 915 MHz, it means the optimized value of l_1 is found to be 4 mm at which $Z_a = 12 + \text{j } 119.6\ \Omega$. As shown in Figure 3B, the impedance matching tuning results at various dipole lengths (l_2) is simulated, and l_2 is increased from 5 to 7 mm in a step of 1 mm. It can be seen that the resistance increases from 9.2 to 15.5 Ω while the reactance remains unchanged at 915 MHz with l_2 increasing. It shows that l_2 mainly controls the real part of impedance by changing the electrical length of antenna. The optimized value of l_2 is 6 mm.

The simulated $|S_{11}|$ responses for different l_1 and l_2 vs frequency are shown in Figure 4A,B, respectively. Here the impedance of R6 chip is substituted into the postprocessing, assuming the chip is bound ideally. The red curve has resonance at 915 MHz with a minimum return loss of −44 dB, which corresponds to the intersections of the resistance and reactance of antenna with the chip at 915 MHz. It indicates that the maximum power transfer from source to antenna is achieved when the antenna impedance is in conjugate matching with the chip. The all optimized parameters are listed in Table 1.

To further investigate the radiation performance of the tag antenna, the simulated surface current distribution at 915 MHz is shown in Figure 5. It can be seen that the current has maximum magnitude across the loop, high current densities are found around the connection between the loop and dipole. Changing the length parameters of the loop and dipole are effective in tuning the impedance and resonant frequency of the antenna, validating the feasibility of the optimization.

4 | EXPERIMENTAL TESTS AND RESULTS

The RFID tags made of graphene-based film are then studied. The measurement results are presented and discussed in this section. A well conjugate complex impedance matching between the antenna and chip only explains that power is transmitted effectively from the antenna to the chip, but it does not confirm that the power is effectively radiated from antenna to free space. The tag realized gain G_t is a key parameter to characterize the radiation efficiency and read range of the tag,[20] and

$$G_t = \frac{P_c}{P_{\text{th}} L_{\text{fwd}}} \tag{2}$$

where P_c is the chip sensitivity, that is, the minimum power needed to wake up the chip, and it is −20 dBm for R6 chip. P_{th} is the measured threshold power, that is, the lowest power from the reader antenna required to activate the tag. L_{fwd} is the forward wireless loss including cable loss and free space loss calculated during calibration of the measurement system. The measurement system is based on backscattering theory. The reader of the RFID measurement system has a linearly polarized patch antenna with an 8 dB gain throughout the frequency range from 800 to 1000 MHz, the transmitted power of the reader ranges from 0 to 27 dBm, and the receiver has a sensitivity level of −75 dBm. The transmitted power is increased in 0.1 dBm steps until the tag is activated, and a valid response to the Electronic Product Code Class 1 Generation 2 protocol's query command is received from the tag.

In theory, G_t can be calculated as:

$$G_t = \text{Gain}\left(1 - |S_{11}|^2\right) \tag{3}$$

where Gain is a mean value of the tag gain. Figure 6A shows the simulated and measured realized gains of the

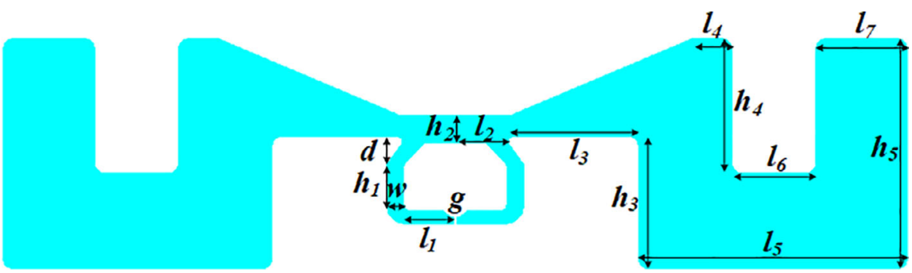

FIGURE 2 Geometry of the proposed tag antenna; the optimized parameters are listed in Table 1

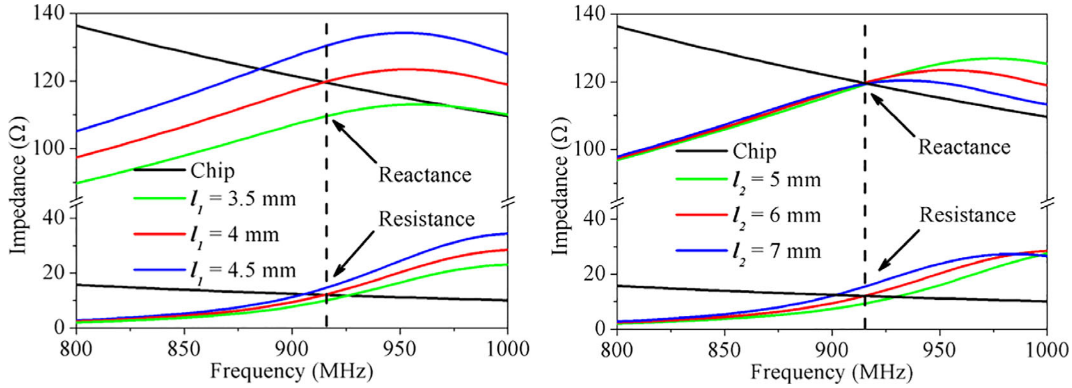

FIGURE 3 Effects of changing the (A) loop length (l_1) and (B) dipole length (l_2) on simulated antennas impedance vs frequency

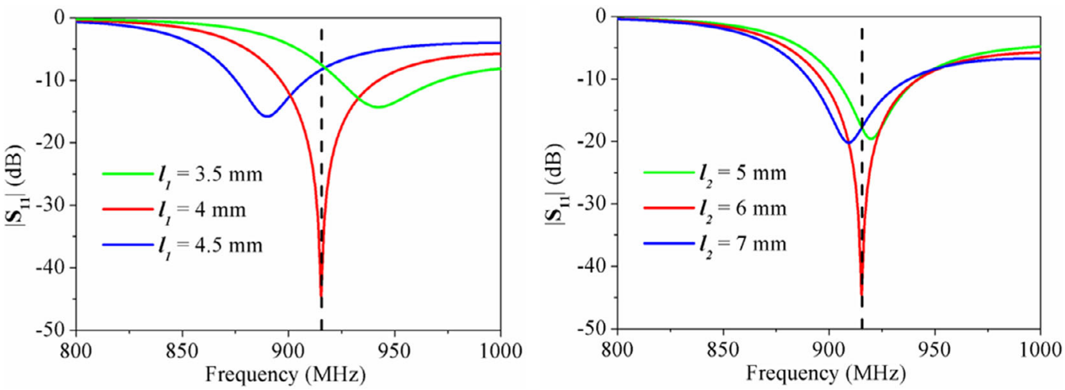

FIGURE 4 Variations of simulated $|S_{11}|$ response of antennas vs frequency for different (A) l_1 and (B) l_2

TABLE 1 Optimized parameters of the proposed antenna

Parameter	l_1	l_2	l_3	l_4	l_5	l_6	l_7	h_1	h_2	h_3	h_4	h_5	d	w	g
Value (mm)	4	6	7.35	14.4	29	9	10	4.7	3	13.8	14	24	2.2	2	0.15

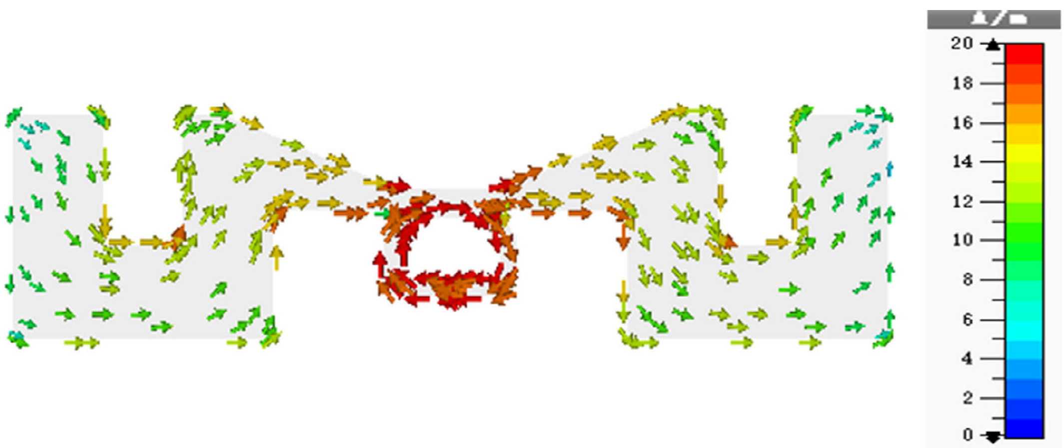

FIGURE 5 Simulated surface current distribution on antenna at 915 MHz

tag vs frequency. A good agreement between the simulated and measured results can be observed. The measured realized gain remains above −1.5 dBi between 860 and 960 MHz, with a peak value around −0.5 dBi at 920 MHz. While the simulated peak realized gain is 0.3 dBi at 915 MHz. The measured peak realized gain is 0.8 dBi lower than the simulated result, as the simulation considers only the ideal impedance matching between the antenna and chip. The reduction includes the loss due to the impedance matching between the antenna and chip in the final assembled tag. There is a 5 MHz frequency shift between the simulated and measured peak realized gain, which may be caused by unavoidable manufacturing tolerance of tag. Figure 6B shows the simulated and measured radiation efficiencies of the tag vs frequency. The measured radiation efficiency ranges from 69% to 93%, and it is beyond 90% in the whole UHF RFID band, which is consistent with the simulation result.

The theoretical tag read range R_t, that is, the maximum distance at which the tag can be read in free space, can be calculated according the Friis formula[21]:

$$R_t = \frac{\lambda}{4\pi}\sqrt{\frac{P_r G_r G_t}{P_t}} = \frac{\lambda}{4\pi}\sqrt{\frac{\mathrm{EIRP}\cdot G_t\cdot\tau}{P_c}} \tag{4}$$

where λ is the wavelength at resonant frequency, P_t, P_r, G_t, and G_r are the radiated power, received power, and realized gains of reader and tag, respectively. EIRP is the equivalent isotropic radiated power, and EIRP $= P_r \times G_r$, $P_c = P_t \times \tau$. It is worth mentioning that G_t in Equation (4) is calculated by Equation (3), when G_t is obtained from Equation (2) by measurements, R_t can be written as:

$$R_t = \frac{\lambda}{4\pi}\sqrt{\frac{\mathrm{EIRP}\cdot\tau}{P_{\mathrm{th}} L_{\mathrm{fwd}}}} \tag{5}$$

The simulated and measured forward theoretical read ranges of the tag vs frequency are shown in Figure 7A. The measured read range greater than 12.3 m from 860 to 960 MHz with a maximum value of 14 m at 920 MHz. The simulated read range is slightly further than the measurement result, since the simulated G_t mentioned above is slightly higher than the measured G_t. As shown in Figure 7B, the case that the simulated gain is higher than the measured value happens in the difference in the radiation patterns in terms of read range of tag at 915 MHz in E-plane. However, both simulated and measured results show consistent variations, and it is evident that these are typical dipole radiation patterns. For comparison, five tags with different l_1 and l_2 are also fabricated and tested, the measured read ranges of the tags vs frequency are shown in Figure 8A,B. The read range of the tag with optimized parameters is far beyond other tags, which illustrates the validity of the optimization. The

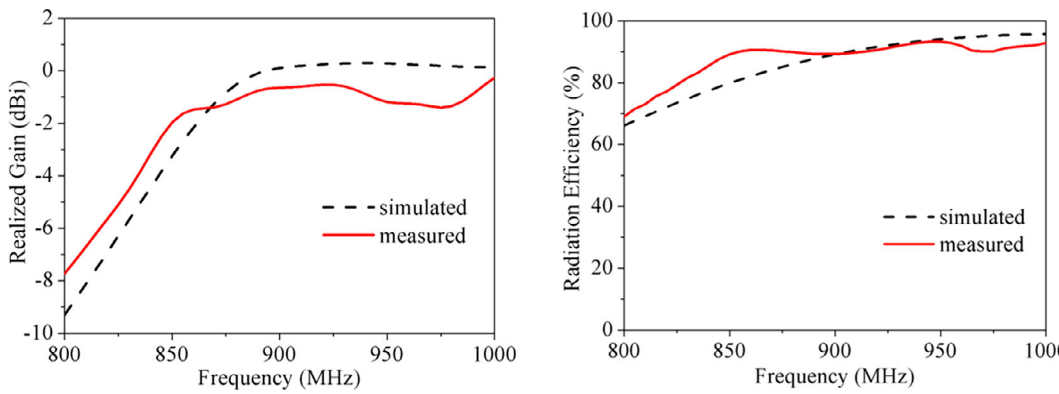

FIGURE 6 Simulated and measured (A) realized gain and (B) radiation efficiency of tag vs frequency

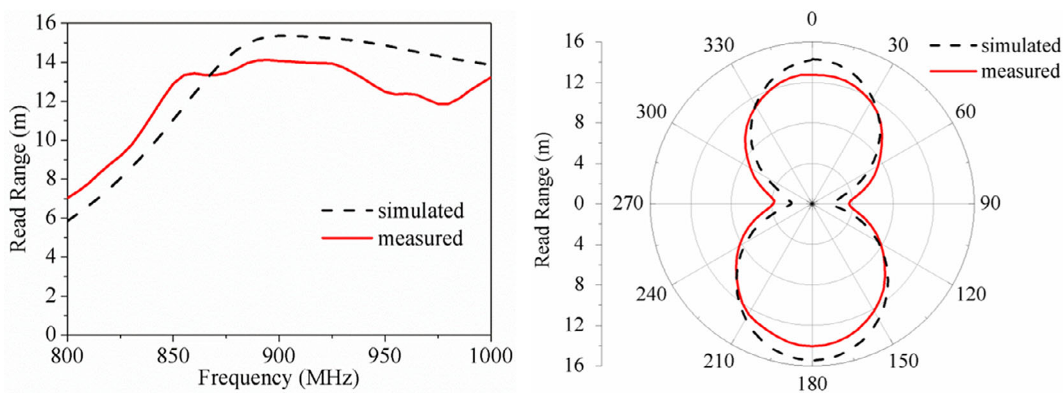

FIGURE 7 Simulated and measured (A) read range of tag vs frequency and (B) radiation patterns in terms of read range of tag at 915 MHz in E-plane

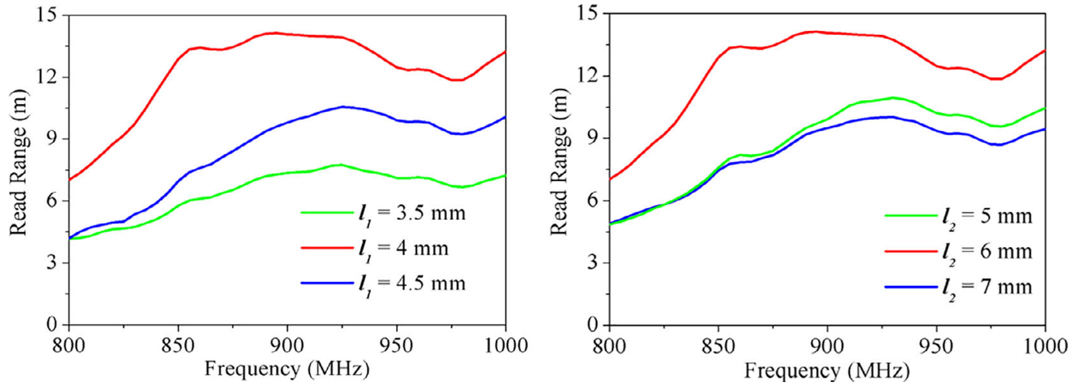

FIGURE 8 Measured read range of tags vs frequency for different (A) l_1 and (B) l_2

TABLE 2 Summary and comparison of the proposed tag and other reported tags

Reference	Material	σ (S m^{-1})	t (μm)	R_s (Ω sq^{-1})	Realized gain (dBi)	Efficiency (%)	Read range (m)
13	Graphene-based inks	4.4×10^3	45	5	Not given	30	4
14	Graphene nanoflakes	4.3×10^4	6	3.8	−4	32	4
15	Graphene laminates	1.39×10^4	38	1.9	−2.18	40	5
16	Graphene-based inks	3.7×10^4	9.4	2.88	Not given	51	9
This article	Graphene-based film	1.1×10^6	30	0.03	−0.5	90	14

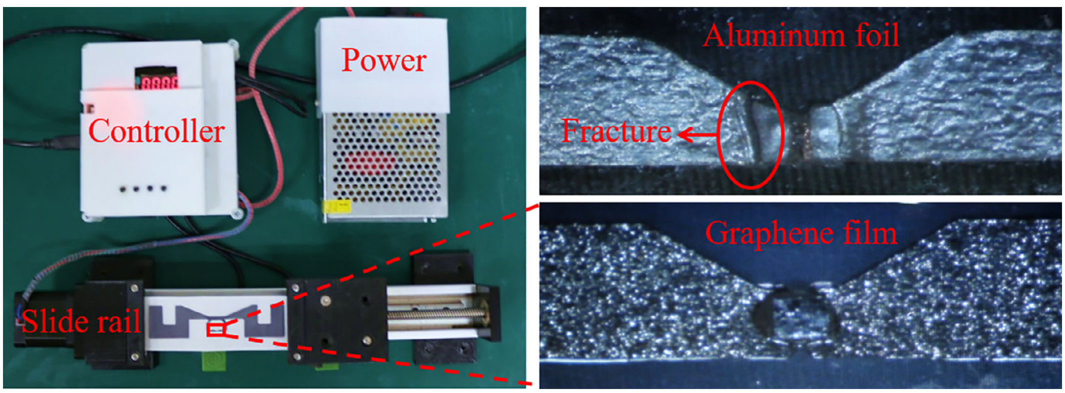

FIGURE 9 A, Top view of the customized device for tag bending and stretching. B, Enlarged images of aluminum foil tag and graphene-based film tag after 300 and 2000 cycles, respectively

material characteristics, realized gain, radiation efficiency, and read range of the proposed tag and are summarized in Table 2 and compared with previously reported tags made of graphene-based composites. Among them, the graphene-based film has the highest conductivity and lowest sheet resistance, contributing the highest radiation efficiency and the longest read range of the tag. The performance of the proposed tag antenna made of graphene-based film is competitive to aluminum etched commercial RFID antennas, such as those in Reference 19.

Next, the flexible property of the tag made of graphene-based film is tested and demonstrated. As shown in Figure 9A, the tag is bended and stretched by a customized device, the controller can adjust the speed of the slide rail and count automatically. The bending with an angle varying from 0° to 90° and back to 0° is denoted as 1 cycle. When the angle is 0°, the tag is flat and stretched by the slide rail, and when it is 90°, the tag is folded. After 2000 cycles, the graphene-based tag is still in good condition, but there is a fracture in the aluminum foil tag in less than 300 cycles, as shown in Figure 9B. The measured read ranges of the graphene-based tag vs frequency at initial state and after 500, 1000, and 2000 cycles are shown in Figure 10A. The read range of graphene-based tag decreases with the increasing cycles due to the weak adhesion between antenna and chip, and the mismatch of impedance degrades the performance of the tag. The graphene-based tag withstands more than 2000 cycles of bending and stretching, and has a read range of 9.5 m at 915 MHz, decreasing by 4.5 m only from the initial state, which indicates remarkable stability of the tag under mechanical

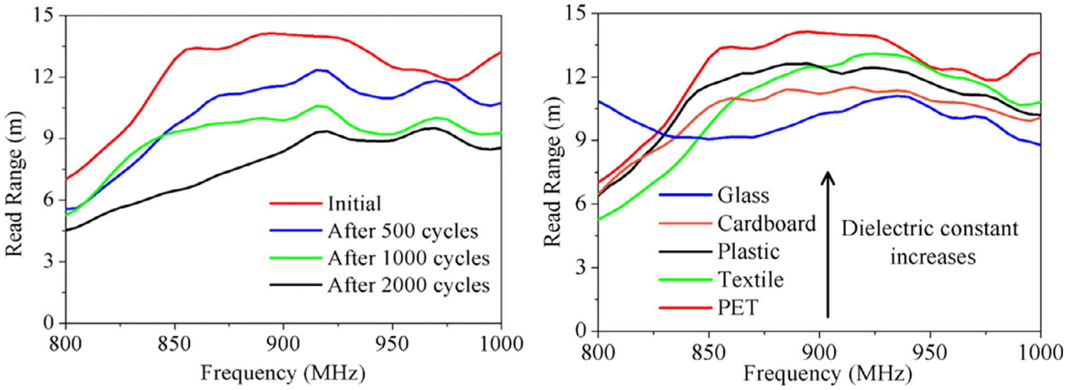

FIGURE 10 A, Measured read range of graphene-based film tag vs frequency at initial state and after 500, 1000, and 2000 cycles. B, Measured read range of graphene-based film tag vs frequency on different substrates

bending. In addition, the measured read ranges of the graphene-based tag vs frequency on different substrates are shown in Figure 10B, including PET, textile, plastic, cardboard, and glass. The read range of tag decreases with the increase of the dielectric constant of the substrate, the read range of tag is greater than 10 m even when placed on glass. It shows the graphene-based film tag can be applied with various scenarios.

5 | CONCLUSIONS

In this article, a long read range and flexible passive UHF RFID tag antenna made of high conductive new graphene-based film has been investigated and tested. The formation of the conductive graphene-based film is made through the thermal treatment of organic polyimide precursor. The design of the tag antenna and the fabrication of the whole tag has been presented in details. The optimal tag has a read range of 14 m with a realized gain of −0.5 dBi and radiation efficiency 93%, due to the high conductive and low sheet resistance of graphene-based film. The performance of graphene-based film tag is superior to other reported graphene-based tags currently. Moreover, the tag can be bended and streched repetitively while the traditional metallic tag would fracture. In addition, the tag can be palced on different substrates for various application scenarios. The proposed tag shows the outstanding characteristics of graphene-based materials and the great potential of using these materials for RFID applications.

ORCID

Daping He https://orcid.org/0000-0002-0284-4990
Zhi P. Wu https://orcid.org/0000-0002-4879-3279

REFERENCES

1. Finkenzeller K. *RFID Handbook: Fundamentals and Applications in Contactless Smart Cards, Radio Frequency Identification and Near-Field Communication*. John Wiley & Sons; 2010.
2. Zhang J, Tian GY, Marindra AM, et al. A review of passive RFID tag antenna-based sensors and systems for structural health monitoring applications. *Sensors*. 2017;17:265.
3. Occhiuzzi C, Caizzone S, Marrocco G. Passive UHF RFID antennas for sensing applications: principles, methods, and classifications. *IEEE Antennas Propag Mag*. 2013;55:14-34.
4. Rao KVS, Nikitin P, Lam S. Antenna design for UHF RFID tags: a review and a practical application. *IEEE Trans Antennas Propag*. 2005;53(12):3870-3876.
5. Skotheim T, Reynolds J. *Handbook of Conducting Polymers*. CRC Press; 2006.
6. Xia Y, Sun K, Ouyang J. Solution-processed metallic conducting polymer films as transparent electrode of optoelectronic devices. *Adv Mater*. 2012;24(18):2436-2440.
7. Rutherglen C, Jain D, Burke P. Nanotube electronics for radio-frequency applications. *Nat Nanotechnol*. 2009;4:811-819.
8. Puchades I, Rossi JE, Cress CD, et al. Carbon nanotube thin-film antennas. *ACS Appl Mater Interfaces*. 2016;8:20986-20992.
9. Geim AK, Novoselov KS. The rise of graphene. *Nat Mater*. 2007;6(3):83-91.
10. Xu Z, Dong X, Bornemann J. Design of a reconfigurable MIMO system for THz communications based on graphene antennas. *IEEE Trans Terahertz Sci Technol*. 2014;4(5):609-617.
11. Huang X, Yin Z, Wu S, Qi X, et al. Graphene based materials: synthesis, characterization, properties, and applications. *Small*. 2011;7(14):1876-1902.
12. Huang X, Leng T, Zhang X, et al. Binder-free highly conductive graphene laminate for low cost printed radio frequency applications. *Appl Phys Lett*. 2015;106(20):2151-2242.
13. Arapov K, Jaakkola K, Ermolov V, et al. Graphene screen-printed radio-frequency identification devices on flexible substrates. *Phys Status Solidi RRL*. 2016;10:812-818.
14. Leng T, Huang X, Chang KH, et al. Graphene nanoflakes printed flexible meandered-line dipole antenna on paper substrate for low-cost RFID and sensing applications. *IEEE Antennas Wirel Propag Lett*. 2016;15:1565-1568.
15. Akbari M, Khan MWA, Hasani M, et al. Fabrication and characterization of graphene antenna for low-cost and environmentally friendly RFID tags. *IEEE Antennas Wirel Propag Lett*. 2016;15:1569-1572.
16. Pan K, Fan YY, Leng T, et al. Sustainable production of highly conductive multilayer graphene ink for wireless connectivity and IoT applications. *Nat Commun*. 2018;9:5197.

17. Song RG, Wang QL, Mao BY, et al. Flexible graphite films with high conductivity for radio-frequency antennas. *Carbon*. 2018;130:164-169.
18. Song RG, Huang GL, Liu CY, et al. High-conductive graphene film based antenna array for 5G mobile communications. *Int J RF Microw Comput Eng*. 2019;29(6):e21692.
19. Smartrac.DOGBONE(MonzaR6&R6P)Datasheet. https://www.smartracgroup.com/files/content/Products_Solutions/PDF/0028_SMARTRAC_DOGBONE.pdf. June 2018.
20. Nikitin P, Rao KVS, Martinez R, et al. Sensitivity and impedance measurements of UHF RFID chips. *IEEE Trans MTT*. 2009;57:1297-1302.
21. Balanis CA. *Antenna Theory: Analysis and Design*. John Wiley & Sons; 2012.

AUTHOR BIOGRAPHIES

Bohan Zhang (corresponding author) received his BSc and MSc degrees from Huazhong University of Science and Technology, Wuhan, China, in 2011, and Wuhan University of Technology, Wuhan, China, in 2014. He is currently pursuing PhD degree in the Hubei Engineering Research Center of RF-Microwave Technology and Application, Wuhan University of Technology, Wuhan, China. His research interests include graphene-based materials, RF and microwave devices design, and Internet of Things techniques.

Xuyang Tang was born in Hubei, China, in 1995. He received the BS degree in Electronic Information Science and Technology from Wuhan University of Technology, Hubei, China, in 2017. He is now pursuing the MS degree at Hubei Engineering Research Center of RF-Microwave Technology and Application, School of Science, Wuhan University of Technology, Wuhan, China. His current research interests emphasize on metal-mountable RFID tag antenna and microstrip antenna.

Jingwei Zhang received the BS degree in electrical engineering from the Wuhan University of Technology, Hubei, China, in 2009 and the PhD degree in electrical engineering and electronics from the University of Liverpool, Liverpool, UK, in 2014. She is now a associate professor in School of Science and Hubei Engineering Research Center of RF-Microwave Technology and Application, Wuhan University of Technology. Her research interests include wireless power transfer and energy harvesting, graphene-based wireless communication, terahertz band communication, and dielectric resonator antennas.

Chengguo Liu is a full professor at Wuhan University of Technology. He obtained his Bachelor of Science degree from Henan University in 1988, his Master of Sience degree from Chengdu University of Science and Technology in 1991, and his PhD degree from Xidian University in 2003. From 2005 to 2008, he was engaged in postdoctoral program at Wuhan University of Technology, and from 2011 to 2014, he was engaged in postdoctoral program at PLA Ordnance College. From 1991 to 2004, he has worked with Chinese Research Institue of Radiowave Propagation. From 2004 to now, he has worked with Wuhan University of Technology. His research interest is in antenna and radio wave propagation, microwave technology, wireless communication technology, and electromagnetic compatibility.

Daping He is a full professor at Wuhan University of Technology. He obtained his PhD degree in Materials Processing Engineering from Wuhan University of Technology in 2013. He was a Postdoctoral Fellow in the University of Science and Technology of China. Then, he joined University of Bath as a Newton International Fellow and University of Cambridge as a Postdoctoral Fellow. His research interest is preparation and application of nanocomposite materials into new energy devices, sensors, and RF microwaves field. He has published over 70 peer-reviewed papers and five Chinese patents.

Zhi P. Wu has over 30 years research experience in microwave engineering, antennas, electromagnetic sensors, and eletromagnetic modeling. His research interests include microwave compoents, circuits and subsystems, microwave sensors, IoT architecture and systems for industrial applications, and so forth.

How to cite this article: Zhang B, Tang X, Zhang J, Liu C, He D, Wu ZP. Long read range and flexible UHF RFID tag antenna made of high conductivity graphene-based film. *Int J RF Microw Comput Aided Eng*. 2020;30:e21993. https://doi.org/10.1002/mmce.21993